

Eurasia Specialized Veterinary Publication

International Journal of Veterinary Research and Allied Science

ISSN:3062-357X

2025, Volume 5, Issue 1, Page No: 84-92 Copyright CC BY-NC-SA 4.0 Available online at: www.esvpub.com/

Initial Development of Microfluidic Platforms for Swine Sperm Sorting: Material Selection, Perfusion Mechanisms, and Flow Dynamics

Zhaobei Cai¹, Takele Tesgera Hurisa², Lezhang Wei¹, Qianqian Chen¹, Qin-Zhe Sun², Jing Chen¹*

¹College of Medical Technology and Engineering, Henan University of Science and Technology, He'nan 471023, China.

²College of Physics, Chongqing University, Chongqing 401331, China.

*E-mail ⊠ Qinzhesun2@163.com

ABSTRACT

Enhancing the efficiency of assisted reproductive technologies (ART) in livestock breeding largely depends on improving semen quality by isolating only the most viable spermatozoa from ejaculates. While microfluidic systems have been widely explored for sperm sorting in humans, similar investigations in boar sperm remain scarce. Moreover, although sperm cells are known to be extremely sensitive to microplastics, the potential cytotoxicity of materials employed in microfluidic chip construction has yet to be addressed. This research aimed to examine the possible harmful influence of common microfluidic fabrication materials on boar sperm and to compare different liquid-handling systems (peristaltic, syringe, and pressuredriven microfluidic flow controllers) at three flow rates (10 μL·min⁻¹, 100 μL·min⁻¹, and 1 mL·min⁻¹). The objective was to generate preliminary insights to support the design of a swinespecific microfluidic sperm-sorting platform. Results indicated that none of the tested materials exhibited adverse effects at any concentration. The control group showed the greatest curvilinear velocity relative to both the peristaltic and pressure-based systems. Among the flow conditions, 10 μL·min⁻¹ yielded the least favorable sperm performance, while 1 mL·min⁻¹ demonstrated no significant difference from the control in any evaluated parameter. Overall, all investigated materials proved compatible with sperm viability, any of the pumps tested could be applied for sperm selection, and a flow rate of 1 mL·min⁻¹ was identified as the most effective for sperm transfer.

Keywords: Microfluidic, Swine, Sperm, Assisted reproductive technologies (ART)

Received: 28 February 2025 Revised: 29 May 2025 Accepted: 01 June 2025

How to Cite This Article: Cai Z, Hurisa TT, Wei L, Chen Q, Sun Q, Chen J. Initial Development of Microfluidic Platforms for Swine Sperm Sorting: Material Selection, Perfusion Mechanisms, and Flow Dynamics. Int J Vet Res Allied Sci. 2025;5(1):84-92. https://doi.org/10.51847/nLsHp9MPXu

Introduction

Assisted reproductive technologies (ART), including artificial insemination (AI), are routinely employed to enhance fertility outcomes in both humans and animals [1–3]. The effectiveness of these technologies is strongly influenced by semen quality. To predict ART success in livestock, semen analysis commonly assesses factors such as sperm concentration, morphology, and motility [4, 5]. Improving ART outcomes in animal reproduction requires refining semen samples by isolating high-quality spermatozoa from each ejaculate. Although numerous techniques have been explored for sperm selection, no universal standard currently exists. Conventional sorting methods are typically based on motility (e.g., swim-up or density gradient centrifugation) or apoptosis detection markers (MACS) [6]. Despite their reliability, these procedures are costly and time-intensive—particularly unsuitable for the large semen volumes typical of boar ejaculates.

Recent research has sought to replicate the sperm-selection process occurring within the female reproductive tract through the application of microfluidic technologies [7]. Most studies on microfluidic-assisted sperm sorting have focused on human semen, and although multiple device prototypes have been reported, their performance requires further optimization. Fertile Chip remains the only commercially tested platform, yet clinical trials revealed no improvement in fertilization rates among couples with unexplained infertility [8]. Microfluidic systems hold promise for simulating the reproductive tract environment to facilitate sperm navigation mechanisms such as rheotaxis, thermotaxis, and chemotaxis [9–11], thereby enabling the selection of morphologically and functionally superior spermatozoa.

Sperm cells are highly vulnerable to numerous environmental agents, including drugs, nanoparticles, and microplastics, all of which can negatively influence motility, morphology, or overall viability [12–14]. Despite extensive work on microfluidic sperm-sorting systems, few have considered the potential toxicity of construction materials. Typical substrates for device fabrication include PDMS (polydimethylsiloxane), PMMA (polymethyl methacrylate), COP/COC (cyclic olefin polymer/copolymer), and PS (polystyrene), while tubing materials often consist of silicone, FEP (fluorinated ethylene propylene), PTFE (polytetrafluoroethylene), or PVC (polyvinyl chloride) [15–17]. Since such materials can influence cellular integrity, cytotoxicity testing remains crucial for ensuring device safety.

Another critical aspect of microfluidic setup design involves the fluid delivery mechanism, which regulates medium perfusion and shear stress to mimic in vivo reproductive conditions. Common flow-control technologies include rocking platforms, peristaltic systems, syringe-driven devices, and pressure-based controllers. Among these, syringe pumps are the most frequently applied for sperm manipulation [18–21]; however, the influence of other systems on sperm performance has not been systematically investigated.

While human studies have explored the use of microfluidics for sperm quality improvement, their application in swine reproduction remains limited. The present study aimed to identify the most appropriate materials for building a boar-specific microfluidic platform and to assess the effects of commonly employed flow-control approaches on sperm characteristics. The outcomes provide essential groundwork for future development of an efficient microfluidic system for selecting high-quality boar sperm.

Materials and Methods

Semen handling

For this study, semen from three adult boars aged 2–5 years was used. The animals, all fertile and exhibiting normal semen traits, were maintained under standard welfare and feeding protocols at a commercial boar semen facility (Semen Cardona stud, Tarazona, Spain). Ejaculates were obtained manually using the glove-hand method. Only samples with \geq 70% motile cells and \geq 75% morphologically normal spermatozoa were processed. Each ejaculate was diluted with Vitasem extender (Magapor, Zaragoza, Spain) to reach a final concentration of 30 × 10^6 spermatozoa per milliliter and preserved at +16 °C.

Experimental layout

Experiment 1 – toxicity screening of microdevice and tubing components.

Three substrates for microdevice fabrication were tested: polydimethylsiloxane (PDMS; Sylgard™ 184 Elastomer Kit), polymethyl methacrylate (PMMA; Clear Acrylic Sheet Panel, Model MCL0016), and cyclo olefin polymer (COP; ZeonorFilm™ ZF 14–188). In parallel, three tubing materials were assessed: polytetrafluoroethylene (PTFE; Darwin Microfluidics, LVF-KTU-15), fluorinated ethylene propylene (FEP; MFLX06406–60), and Tygon (PVC-based; E-3603). For each tested material, 1 cm × 1 cm fragments were cut and placed in 15 ml of semen at three inclusion levels (1, 5, or 10 pieces). Sperm attributes were analyzed following 24 h and 72 h of incubation.

Experiment 2 – evaluation of different flow-driving mechanisms and flow rates.

This part compared three fluid delivery systems—peristaltic pump, syringe pump, and microfluidic flow controller—operating at 10 μl min⁻¹, 100 μl min⁻¹, and 1 ml min⁻¹, with measurements taken at 5, 15, 30 minutes, and 1 hour. The tested equipment included a peristaltic pump (Reglo Digital Pump, 4-Channel 12-Roller, Masterflex Ismatec), a syringe pump (NE-1600 Six-Channel Programmable Syringe Pump, Pump Systems Inc.),

and a microfluidic flow controller (Flow EZ 1000 mbar, Fluigent) equipped with a flow sensor (Flow Unit M, Fluigent).

In both peristaltic and perfusion setups, semen samples were transferred into tubes (188–271, Cellstar) connected to the pumps through tubing, and the outflow was collected in a receiving container. For syringe-based operation, semen was loaded into syringes (5200-000 V0, HENKE-JECT) and recovered after passage. Flow conditions of 10 µl min⁻¹, 100 µl min⁻¹, and 1 ml min⁻¹ were applied. Assessments were carried out after 5, 15, 30 minutes, and 1 hour of exposure.

Assessment of sperm characteristics

Motility analysis

To quantify motility, 2 μ l of each semen aliquot was mounted on a disposable counting chamber (Life Optic Slide, 20 μ m depth) and observed using a computer-assisted sperm analyzer (CASA; ISAS System, Spain) at 37 °C with negative-phase contrast microscopy under $10\times$ magnification. Dilution was adjusted to visualize roughly 100-120 sperm per field, examining four fields (\approx 400 cells total) at 30 frames per second. Particles between 13 and 101 μ m were classified as spermatozoa. The CASA system recorded total motility (TM), progressive motility (PM), and motion kinematic variables including: VCL (curvilinear velocity, μ m s⁻¹), VSL (straight-line velocity, μ m s⁻¹), VAP (average path velocity, μ m s⁻¹), LIN (linearity, %), STR (straightness, %), WOB (wobble index, %), ALH (amplitude of lateral head movement, μ m), and BCF (beat-cross frequency, Hz). Progressive motion was defined as STR > 70% and VAP > 40 μ m s⁻¹.

Morphology and viability

Sperm integrity and survival were assessed with eosin–nigrosin staining as described by Bernard *et al.* (2019) [22]. Equal drops of semen and stain were combined, smeared on a slide, air-dried, and inspected microscopically. Two hundred cells were counted per slide to determine the frequency of head, midpiece, or tail malformations and the occurrence of cytoplasmic droplets. Cells remaining unstained were classified as viable, while stained ones were labeled non-viable. Percentages of normal and living spermatozoa were calculated accordingly.

Statistical Processing

Data analysis was conducted using SPSS Statistics v19.0. A General Linear Model (GLM) followed by Duncan's multiple-range post-hoc test was employed to detect factor interactions. Significance was assigned when P < 0.05 (* P < 0.05; *** P < 0.01; **** P < 0.001). Values are presented as mean \pm standard deviation.

Results and Discussion

Experiment 1

In total, three device materials (PDMS, PMMA, COP), three tubing materials (TYGON, PTFE, FEP), and three dosage levels were tested (**Figure 1**). Sperm samples were incubated with each substrate, and their parameters were measured after 24 h and 48 h (**Table 1**). None of the tested materials produced measurable adverse effects at any concentration. After 24 h, FEP caused a temporary decline in the BCF parameter, which normalized after 48 h of incubation (**Figure 2**).

Table 1. Influence of tested materials on sperm characteristics after 24 h and 48 h of contact. Mean \pm SD values are shown. Significant threshold: * < 0.05.

Parameter	Control	Device: PDMS	Device: PMMA	Device: COP	Tubing: PVC (Tygon)	Tubing: PTFE	Tubing: FEP	p-value
	24 h	48 h	24 h	48 h	24 h	48 h	24 h	48 h
TM	49.00 ±	60.60 ±	47.11 ±	51.14 ±	38.12 ± 12.41	51.18 ±	47.87 ±	58.91 ±
	17.07	1.50	11.31	10.74		10.15	12.15	7.92
PM	$38.86 \pm$	41.10 ±	35.61 ±	34.97 ±	29.53 ± 11.03	34.37 ±	38.71 ±	42.15 ±
	14.97	6.05	8.91	7.85		8.55	10.86	5.91
VCL	54.01 ±	87.78 ±	61.06 ±	85.34 ±	60.41 ± 9.74	87.34 ±	64.39 ±	90.21 ±
	6.94	8.88	11.81	9.80		11.44	7.81	10.57
VSL	29.18 ±	47.70 ±	31.65 ±	45.09 ±	29.18 ± 7.31	46.18 ±	34.91 ±	49.13 ±
	1.86	7.00	5.04	4.48		7.85	6.76	3.79

VAP	36.86 ±	68.67 ±	41.13 ±	62.81 ±	38.37 ± 7.64	64.97 ±	43.39 ±	68.25 ±
VAP	2.20	3.20	7.33	6.23	38.37 ± 7.04	7.23	7.97	6.22
LIN	54.42 ±	54.41 ±	52.52 ±	53.20 ±	48.42 ± 9.01	52.74 ±	54.06 ±	57.74 ±
LIIN	5.25	7.18	6.66	5.85	40.42 ± 9.01	5.24	6.89	3.40
STR	$79.26 \pm$	$69.34 \pm$	$77.30 \pm$	$71.93 \pm$	75.62 ± 6.08	$70.78 \pm$	80.37 ±	72.12 ±
SIK	2.53	8.64	4.00	4.81	75.02 ± 0.08	7.13	3.49	4.09
WOB	$68.58 \pm$	$78.51 \pm$	67.75 ±	$73.94 \pm$	63.56 ± 6.95	$74.59 \pm$	67.11 ±	75.89 ±
WOB	4.91	4.13	5.93	6.34		3.34	6.38	3.38
ALH	2.36 ±	$3.167 \pm$	$2.58 \pm$	3.41 ±	2.61 ± 0.37	$3.37 \pm$	2.65 ±	3.42 ±
ALII	0.37	0.72	0.47	0.69	2.01 ± 0.57	3.37 ± 0.62	0.28	0.60
BCF	8.46 ±	7.93 ±	8.45 ±	7.60 ±	8.65 ± 0.45 ab	7.70 ±	8.80 ±	7.76 ±
БСГ	0.50ab	0.68	0.49ab	0.51	6.03 ± 0.4340	$\begin{array}{ccccc} 52.74 \pm & 54.06 \pm \\ 5.24 & 6.89 \\ \hline 70.78 \pm & 80.37 \pm \\ 7.13 & 3.49 \\ \hline 74.59 \pm & 67.11 \pm \\ 3.34 & 6.38 \\ \hline 3.37 \pm & 2.65 \pm \\ 0.62 & 0.28 \\ \hline 7.70 \pm & 8.80 \pm \\ 0.32 & 0.37 ab \\ \hline 84.99 \pm & 85.12 \pm \\ 5.32 & 4.12 \\ \hline \end{array}$	0.37ab	0.40
VIT	85.36 ±	86.24 ±	84.36 ±	85.17 ±	85.99 ± 3.23	84.99 ±	85.12 ±	85.21 ±
V11	4.33	4.13	4.22	4.19	63.99 ± 3.23	5.32 4.1	4.12	4.27
МА	$22.33 \pm$	$22.67 \pm$	$22.19 \pm$	21.23 ±	22.99 ± 1.56	22.56 ±	21.44 ±	23.34 ±
MA	1.67	1.23	1.2	1.87		1.37	1.02	1.99

TM = total motility (%); PM = progressive motility (%); VCL = curvilinear velocity (μ m s⁻¹); VSL = straight-line velocity (μ m s⁻¹); LIN = linearity (%); STR = straightness (%); WOB = wobble index (%); ALH = lateral head displacement (μ m); BCF = beat-cross frequency (Hz); VIT = vitality (%); morphological abnormalities (%).

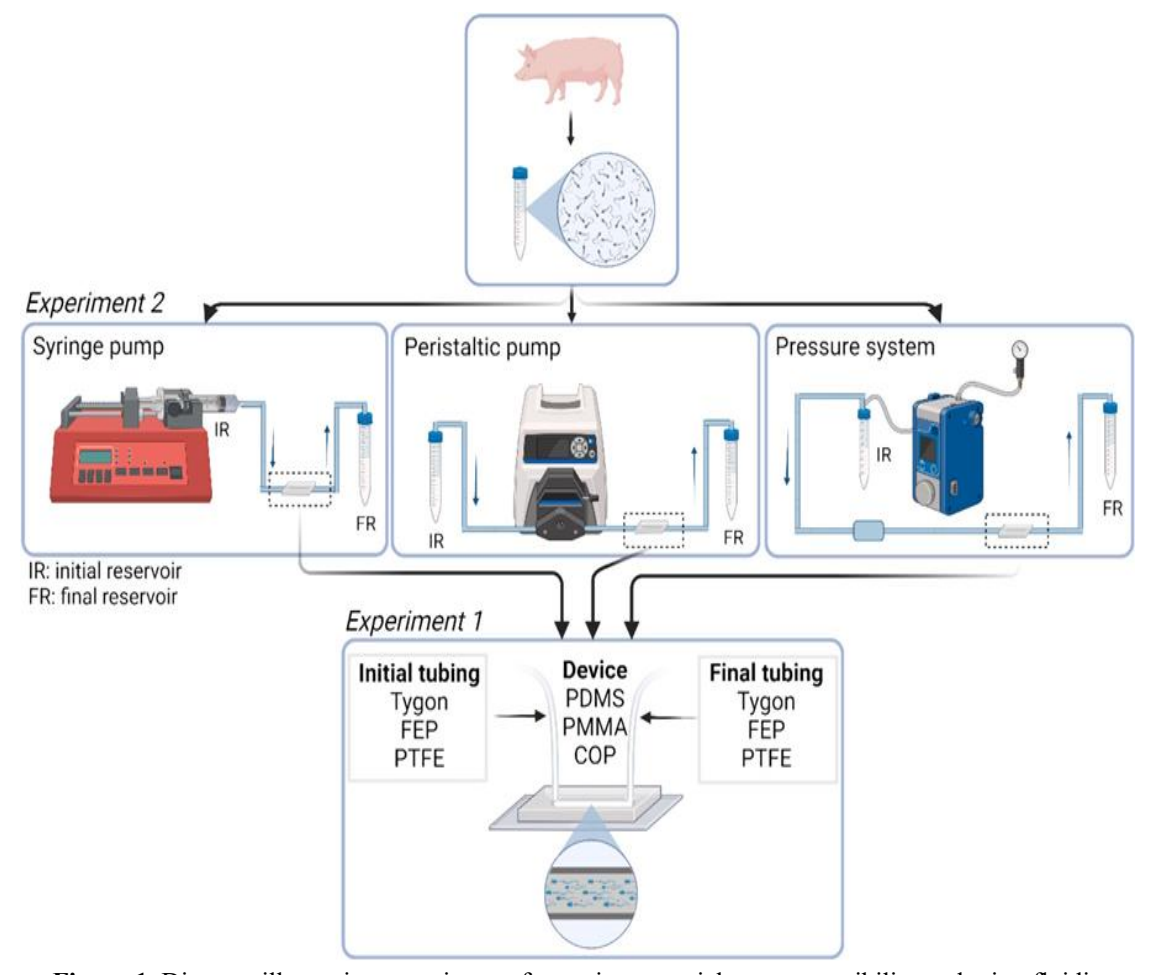


Figure 1. Diagram illustrating experiments for testing material cytocompatibility and microfluidic configurations. PDMS, PMMA, and COP were assessed for chip fabrication, while PVC (Tygon), FEP, and PTFE served as tubing candidates. Experiment 2 tested flow systems at varied rates and durations. Figure generated using BioRender.

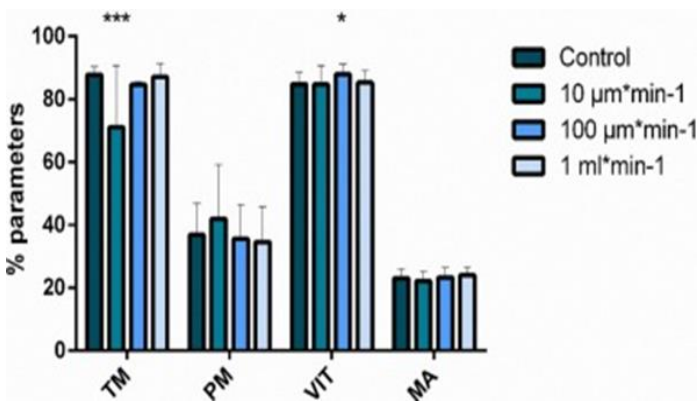


Figure 2. Comparison of total motility (TM), progressive motility (PM), vitality (VIT), and morphological abnormalities (MA) under different flow conditions. Data are expressed as mean \pm standard deviation. Statistical relevance: *** < 0.001; * < 0.05.

Experiment 2

Three distinct fluid propulsion systems—peristaltic pump, syringe pump, and pressure-driven setup—were evaluated at various flow rates and exposure durations (**Figure 1**). When comparing the systems used to circulate the semen samples, a significant difference was observed only in VCL values, with the control group exhibiting higher readings than both the peristaltic and pressure-based configurations (**Table 2**).

Regarding flow intensity, the control and 1 ml·min⁻¹ rate did not differ significantly across any evaluated parameters. However, a flow rate of 100 μ l·min⁻¹ resulted in notably reduced values for VIT, VAP, and BCF, while the lowest overall performance was detected at 10 μ l·min⁻¹ (**Table 3**). Across the measurement period, TM, PM, VIT, and MA remained consistent. Interaction effects between pumping system and flow rate were significant for TM (p = 0.009) and VIT (p = 0.003). Specifically, both parameters decreased under the 10 μ l·min⁻¹ condition when using pressure-based or peristaltic mechanisms, whereas no variation among flow rates was observed with the syringe pump. These patterns are likely associated with the distinct operational dynamics of each pumping method.

Semen samples were subsequently circulated for 5, 15, 30 minutes, and 1 hour. No statistical differences were identified in total motility, progressive motility, vitality, or morphological abnormality percentages (TM, PM, VIT, MA) across the four exposure times (Figure 3). Similarly, parameters such as VCL, VSL, LIN, STR, WOB, ALH, and BCF showed no significant variation at any time point.

Table 2. Influence of pumping system type on sperm characteristics. Data expressed as mean \pm standard deviation. Significance level: * < 0.05.

Parameter	Baseline	Syringe System	Peristaltic System	Pressure Mechanism	p-value
TM	87.78 ± 2.54	84.60 ± 4.34	80.73 ± 17.29	81.88 ± 13.94	0.125
PM	36.90 ± 9.91	35.37 ± 13.41	34.58 ± 11.68	41.22 ± 13.24	0.053
VCL	$101.92 \pm 4.48a$	86.76 ± 17.39 ab	$83.05 \pm 23.73b$	$81.71 \pm 25.02b$	0.044*
VSL	35.98 ± 6.99	28.86 ± 7.91	28.29 ± 8.28	30.76 ± 9.50	0.986
VAP	81.68 ± 1.81	65.29 ± 18.67	63.71 ± 22.25	62.56 ± 23.22	0.131
LIN	35.50 ± 7.86	33.76 ± 9.25	35.19 ± 8.90	38.83 ± 9.95	0.057
STR	44.10 ± 9.03	46.04 ± 12.04	47.42 ± 12.67	52.23 ± 12.21	0.195
WOB	80.20 ± 2.27	74.08 ± 10.17	75.02 ± 8.89	74.75 ± 11.11	0.666
ALH	2.92 ± 0.34	2.65 ± 0.45	2.58 ± 0.56	2.54 ± 0.58	0.287
BCF	7.38 ± 0.65	8.10 ± 1.01	7.75 ± 0.64	7.85 ± 0.79	0.107
VIT	84.80 ± 3.83	86.37 ± 4.83	85.97 ± 5.62	85.71 ± 2.32	0.292
MA	23.80 ± 3.12	22.10 ± 2.12	23.15 ± 2.12	24.01 ± 3.56	0.899

TM: total motility (%); PM: progressive motility (%); VCL: curvilinear velocity (μm/s); VSL: straight-line velocity (μm/s); LIN: linearity (%); STR: straightness (%); WOB: wobble index (%); ALH: lateral head displacement (μm); BCF: beat-cross frequency (Hz); VIT: vitality (%); MA: morphological abnormalities (%).

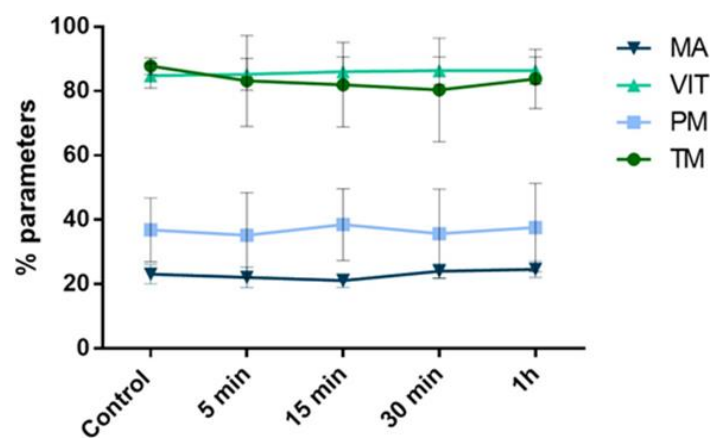


Figure 3. Comparative evaluation of total motility (TM), progressive motility (PM), vitality (VIT), and morphological abnormalities (MA) of sperm samples exposed to varying flow durations.

Table 3. Impact of flow rate on sperm kinematic and morphological parameters. Results shown as mean \pm standard deviation. Statistical thresholds: *** < 0.001; ** < 0.01; * < 0.05.

Parameter	Baseline	1 mL/min	10 μL/min	100 μL/min	p-value
VCL	$101.92 \pm 4.48a$	$98.88 \pm 13.96a$	$59.99 \pm 17.80b$	$84.22 \pm 17.95a$	<0.001***
VSL	$35.98 \pm 6.99a$	$33.36 \pm 6.19a$	$22.03 \pm 6.09b$	$29.56 \pm 8.95ab$	<0.001***
VAP	81.68 ± 1.81a	78.93 ± 10.70 ab	40.71 ± 13.65c	63.74 ± 19.91b	<0.001***
LIN	35.50 ± 7.89	34.60 ± 9.08	39.03 ± 12.67	34.88 ± 7.12	0.095
STR	$44.10 \pm 9.03b$	$42.82 \pm 9.37b$	58.13 ± 16.66a	$47.64 \pm 8.22ab$	<0.001***
WOB	$80.20 \pm 2.27a$	$80.07 \pm 4.91a$	67.18 ± 8.17 b	74.00 ± 11.28 ab	<0.001***
ALH	$2.92 \pm 0.34a$	$2.79 \pm 0.61a$	$2.19 \pm 0.29b$	$2.64 \pm 0.42 ab$	<0.001***
BCF	$7.38 \pm 0.65a$	$7.53 \pm 0.61 ab$	$7.96 \pm 0.59 ab$	$8.19 \pm 0.99 b$	0.002**

VCL: curvilinear velocity (μm/s); VSL: straight-line velocity (μm/s); LIN: linearity (%); STR: straightness (%); WOB: wobble index (%); ALH: lateral head displacement (μm); BCF: beat-cross frequency (Hz).

The selection of an appropriate substrate represents the first critical step in the fabrication of any microfluidic platform, as the optimal choice depends on the intended experimental purpose and technical requirements. Since the introduction of this technology for cell culture applications nearly twenty years ago, a wide range of materials with distinct properties has been employed to construct microfluidic chips [16]. Among them, polymer-derived materials remain the most frequently used due to their surface adaptability for biomedical research and compatibility with living cells [15].

To date, no previous work has directly compared the influence of three fabrication materials (PDMS, PMMA, COP), three tubing compositions (TYGON, PTFE, FEP), and their respective concentration levels on sperm performance. Our findings indicate that all these materials—commonly adopted in microfluidic engineering—are appropriate for sperm processing. PDMS, in particular, is the most extensively utilized elastomer in this field because of its low cost, ease of molding into complex geometries, and gas permeability, which ensures proper oxygen exchange in culture media. Nonetheless, PDMS presents several drawbacks: its hydrophobic nature requires surface modification to support cell attachment, and its porous structure leads to absorption of small organic molecules and lipids from the surrounding medium [17, 23].

Thermoplastics such as PMMA and COP have recently gained attention due to their excellent optical transparency, high chemical resistance—even to polar solvents—low autofluorescence, and reduced molecular adsorption. They also allow large-scale production through injection molding at a low unit cost, providing a robust option for industrial-scale device manufacturing [22, 24]. Numerous microfluidic devices built from these materials have been applied to sperm manipulation and assessment, showing consistent suitability for such purposes [8, 9, 25–27]. Our data align with those observations, as none of the tested materials negatively impacted the sperm parameters analyzed.

The tubing material also plays a crucial role in assembling microfluidic circuits, as it links the different system components. In this investigation, tubing made of PVC (Tygon), FEP, and PTFE was examined, and similar to the chip materials, none exhibited adverse effects on sperm quality. Eravuchira *et al.* (2018) successfully used Tygon tubing for single-sperm selection, demonstrating that regulation of flow velocity could isolate sperm with normal morphology [19]. Historically, most microfluidic studies in sperm research have been conducted under static conditions, eliminating the need for continuous flow or tubing connections. In contrast, our findings confirm that all tested tubing types are safe for use in flow-based setups, showing no cytotoxic or mechanical harm to spermatozoa.

In this work, three flow application systems—peristaltic pump, syringe pump, and pressure-driven controller—were analyzed under varying flow rates and durations. As literature on dynamic sperm handling is scarce, most prior research has used static culture conditions. The peristaltic pump remains one of the most common methods to generate flow through microfluidic channels, moving fluid by compressing flexible tubing with rotating rollers [28–30]. This produces a pulsating rather than linear stream. The syringe pump, by contrast, is a simple, low-cost instrument requiring minimal auxiliary components [31]. Pressure-driven systems apply a steady air pressure to drive the medium continuously through the circuit, resulting in smooth, laminar flow. These systems enable real-time flow-rate monitoring and pressure control between reservoirs. However, they may pose technical challenges: thermal output from flow sensors can locally heat the fluid, and viscous samples can obstruct the sensors, affecting accuracy.

Previous studies using sperm microfluidics commonly relied on syringe pumps to control flow rate [9, 19, 20]. Our data revealed no significant variation in sperm motility or viability among the three systems, suggesting that all can be effectively used for sperm propulsion. However, shear stress—defined as the tangential force generated by liquid flow over a surface—must be considered when designing microfluidic devices [32]. This phenomenon can occur both within the tubing and inside the microchannels themselves. Although shear stress was not directly quantified in this preliminary study, future research should examine its influence on sperm functionality in greater detail.

Our findings indicate that fluid movement within microfluidic systems, especially at rates approaching 1 ml·min⁻¹, can affect sperm performance. Specifically, the lowest rate tested (10 µl·min⁻¹) in both the peristaltic and pressure-based configurations led to diminished sperm quality. This outcome may stem from the mechanical nature of the devices. The peristaltic pump operates by compressing tubing with rollers, producing forward-and-backward pulsations that intensify at lower speeds. In pressure-driven controllers, heat generated by the flow sensor may expose the sample to localized temperature increases, especially when the flow is slow. Consequently, among the tested systems, the syringe pump appears to be the most reliable choice for consistent, gentle sample handling. Semen was circulated through each setup for 5, 15, 30 minutes, and 1 hour. No significant differences were detected in sperm quality across these time points. This finding is relevant because boar ejaculates have high volume, meaning that sorting or processing often requires extended operation times compared with human or other mammalian samples.

Conclusion

This study demonstrated that the materials most commonly used for microfluidic chip construction (PDMS, PMMA, COP) and tubing assembly (TYGON, PTFE, FEP) do not exhibit cytotoxic effects on spermatozoa. Furthermore, the three tested propulsion methods—syringe pump, peristaltic pump, and pressure-based perfusion system—were all functional for sperm transport. The syringe pump consistently produced the most stable results across all tested flow rates, whereas both peristaltic and pressure-driven systems showed reduced VCL at 10 μl·min⁻¹.

A flow velocity of approximately 1 ml·min⁻¹ is recommended for boar semen applications, as it facilitates faster processing of large ejaculate volumes while minimizing handling stress and potential cellular damage. Together, these results establish the groundwork for designing an integrated microfluidic setup optimized for porcine sperm separation. Future work should focus on refining microfluidic designs and validating new technologies that enable precise, efficient, and safe manipulation of sperm samples.

Acknowledgments: None

Conflict of Interest: None

Financial Support: None

Ethics Statement: None

References

- 1. Tournaye H. Management of male infertility by assisted reproductive technologies. Best Pract Res Clin Endocrinol Metab. 2000;14(3):423–35. doi:10.1053/beem.2000.0089
- 2. Navarro-Rubio S, Güell F. Understanding the correlation between artificial insemination and offspring health outcomes. Birth Defects Res. 2020;112(1):7–18. doi:10.1002/bdr2.1617
- 3. Mellagi APG, Will KJ, Quirino M, Bustamante-Filho IC, da Ulguim RR, Bortolozzo FP. Update on artificial insemination: semen, techniques, and sow fertility. Mol Reprod Dev. 2023;90(7):601–11. doi:10.1002/mrd.23643
- 4. Roldan ERS. Assessments of sperm quality integrating morphology, swimming patterns, bioenergetics and cell signalling. Theriogenology. 2020;150:388–95. doi:10.1016/j.theriogenology.2020.02.017
- 5. Abah KO, Fontbonne A, Partyka A, Nizanski W. Effect of male age on semen quality in domestic animals: potential for advanced functional and translational research? Vet Res Commun. 2023;47(3):1125–37. doi:10.1007/s11259-023-10159-1
- 6. Xie Y, Xu Z, Wu Z, Hong L. Sex manipulation technologies progress in livestock: a review. Front Vet Sci. 2020;7:481. doi:10.3389/fvets.2020.00481
- 7. Jahangiri AR, Ziarati N, Dadkhah E, Bucak MN, Rahimizadeh P, Shahverdi A, et al. Microfluidics: the future of sperm selection in assisted reproduction. Andrology. 2023;1:1–17. doi:10.1111/ANDR.13578
- 8. Yetkinel S, Kilicdag EB, Aytac PC, Haydardedeoglu B, Simsek E, Cok T. Effects of the microfluidic chip technique in sperm selection for intracytoplasmic sperm injection for unexplained infertility: a prospective, randomized controlled trial. J Assist Reprod Genet. 2019;36(3):403–9. doi:10.1007/s10815-018-1375-2
- 9. Zaferani M, Cheong SH, Abbaspourrad A. Rheotaxis-based separation of sperm with progressive motility using a microfluidic corral system. Proc Natl Acad Sci USA. 2018;115(33):8272–7. doi:10.1073/pnas.1800819115
- 10. Ko YJ, Maeng JH, Lee BC, Lee S, Hwang SY, Ahn Y. Separation of progressive motile sperm from mouse semen using on-chip chemotaxis. Anal Sci. 2012;28(1):27–32. doi:10.2116/analsci.28.27
- 11. Nagata MP, Endo K, Ogata K, Yamanaka K, Egashira J, Katafuchi N, et al. Live births from artificial insemination of microfluidic-sorted bovine spermatozoa characterized by trajectories correlated with fertility. Proc Natl Acad Sci USA. 2018;115(14):E3087–96. doi:10.1073/pnas.1717974115
- 12. Pérez-Duran F, Acosta-Torres LS, Serrano-Díaz PN, Toscano-Torres IA, Olivo-Zepeda IB, García-Caxin E, et al. Toxicity and antimicrobial effect of silver nanoparticles in swine sperms. Syst Biol Reprod Med. 2020;66(4):281–9. doi:10.1080/19396368.2020.1754962
- 13. D'Angelo S, Meccariello R. Microplastics: a threat for male fertility. Int J Environ Res Public Health. 2021;18(5):1–11. doi:10.3390/ijerph18052392
- 14. Chen Q, Li L, Zhao J, Zhang Y, Xue X. Graphene oxide had adverse effects on sperm motility and morphology through oxidative stress. Toxicol In Vitro. 2023;92:1–9. doi:10.1016/j.tiv.2023.105653
- 15. Gencturk E, Mutlu S, Ulgen KO. Advances in microfluidic devices made from thermoplastics used in cell biology and analyses. Biomicrofluidics. 2017;11(5):1–41. doi:10.1063/1.4998604
- 16. Ren K, Zhou J, Wu H. Materials for microfluidic chip fabrication. Acc Chem Res. 2013;46(11):2396–406. doi:10.1021/ar300314s
- 17. Van Midwoud PM, Janse A, Merema MT, Groothuis GMM, Verpoorte E. Comparison of biocompatibility and adsorption properties of different plastics for advanced microfluidic cell and tissue culture models. Anal Chem. 2012;84(9):3938–44. doi:10.1021/ac300771z
- 18. Ahmadkhani N, Saadatmand M, Kazemnejad S, Abdekhodaie MJ. Qualified sperm selection based on the rheotaxis and thigmotaxis in a microfluidic system. Biomed Eng Lett. 2023;13(4):671–80. doi:10.1007/s13534-023-00294-8

- 19. Eravuchira PJ, Mirsky SK, Barnea I, Levi M, Balberg M, Shaked NT. Individual sperm selection by microfluidics integrated with interferometric phase microscopy. Methods. 2018;136:152–9. doi:10.1016/j.ymeth.2017.09.009
- 20. Ghassemi Panah A, Zabetian Targhi M, Heydari A, Halvaei I. A novel microfluidic system to separate sperm using spermatozoa inherent motion and inertial effect. J Biomech. 2022;142:1–6. doi:10.1016/j.jbiomech.2022.111256
- 21. Agarwal A, Gupta S, Sharma R. Eosin-Nigrosin staining procedure. In: Andrological Evaluation of Male Infertility. Springer, Cham; 2016. p. 73–7. doi:10.1007/978-3-319-26797-5 8
- 22. Bernard M, Jubeli E, Bakar J, Saunier J, Yagoubi N. Impact of simulated biological aging on physicochemical and biocompatibility properties of cyclic olefin copolymers. Mater Sci Eng C. 2019;97:377–87. doi:10.1016/j.msec.2018.12.032
- 23. Mehling M, Tay S. Microfluidic cell culture. Curr Opin Biotechnol. 2014;25:95–102. doi:10.1016/j.copbio.2013.10.005
- 24. Nunes PS, Ohlsson PD, Ordeig O, Kutter JP. Cyclic olefin polymers: emerging materials for lab-on-a-chip applications. Microfluid Nanofluid. 2010;9(2–3):145–61. doi:10.1007/S10404-010-0605-4/FIGURES/7
- 25. Shirota K, Yotsumoto F, Itoh H, Obama H, Hidaka N, Nakajima K, et al. Separation efficiency of a microfluidic sperm sorter to minimize sperm DNA damage. Fertil Steril. 2016;105(2):315–21. doi:10.1016/j.fertnstert.2015.10.023
- 26. Quinn MM, Jalalian L, Ribeiro S, Ona K, Demirci U, Cedars MI, et al. Microfluidic sorting selects sperm for clinical use with reduced DNA damage compared to density gradient centrifugation with swim-up in split semen samples. Hum Reprod. 2018;33(8):1388–93. doi:10.1093/humrep/dey239
- 27. Zhang X, Khimji I, Gurkan UA, Safaee H, Catalano PN, Keles HO, et al. Lensless imaging for simultaneous microfluidic sperm monitoring and sorting. Lab Chip. 2011;11(15):2535–40. doi:10.1039/c1lc20236g
- 28. Essig M, Friedlander G. Tubular shear stress and phenotype of renal proximal tubular cells. J Am Soc Nephrol. 2003;14(90001):33S-35. doi:10.1097/01.ASN.0000067650.43083.DF
- 29. Baudoin R, Griscom L, Monge M, Legallais C, Leclerc E. Development of a renal microchip for in vitro distal tubule models. Biotechnol Prog. 2007;23(5):1245–53. doi:10.1021/BP0603513
- 30. Maggiorani D, Dissard R, Belloy M, Saulnier-Blache JS, Casemayou A, Ducasse L, et al. Shear stress-induced alteration of epithelial organization in human renal tubular cells. PLoS One. 2015;10(7). doi:10.1371/journal.pone.0131416
- 31. Ross EJ, Gordon ER, Sothers H, Darji R, Baron O, Haithcock D, et al. Three dimensional modeling of biologically relevant fluid shear stress in human renal tubule cells mimics in vivo transcriptional profiles. Sci Rep. 2021;11(1):1–14. doi:10.1038/s41598-021-93570-5
- 32. Hamacher T, Berendsen JTW, Kruit SA, Broekhuijse MLWJ, Segerink LI. Effect of microfluidic processing on the viability of boar and bull spermatozoa. Biomicrofluidics. 2020;14(4):1–8. doi:10.1063/5.0013919